CIMAC CONGRESS 25
ZURICH, MAY 19 – 23, 2025

2025 | 308

Exploration of novel combustion strategies for alternative fuels using computational fluid dynamics

Fuels - Alternative & New Fuels

James Wood, Woodward Inc.

Nolan Polley, Woodward Inc.
Gregory Hampson, Woodward Inc.

ABSTRACT

To reduce global carbon emissions, transitioning industries such as power generation and marine transportation from traditional carbon-based fuels to non-carbon or carbon-neutral fuels is critical. However, current zero-carbon and carbon-neutral fuel properties and combustion behavior deviate from traditional carbon-based fuels for which internal combustion engines have been optimized. This paper explores, through computational fluid dynamic (CFD), adaptation of optimized combustion strategies for two commonly discussed Power-to-X (P2X) fuels, methanol and ammonia, on a simulated modified diesel engine.

Combustion optimization for two P2X fuels is conducted. In the first case, methanol will be injected and combusted in a conventional dual-fuel strategy with diesel pilot ignition. In the second case, reactivity controlled compression ignition (RCCI) is used with ammonia as the low-reactivity fuel and diesel as the high-reactivity fuel. The goals of the study are to show engine thermal efficiency equal or better than the original diesel configuration and to show the viability of the P2X fuels when used in an optimized combustion system.

This paper focuses on the optimization of the fuel delivery for these alternative fuels. Through CFD modeling, the base engine's "breathing" and fuel delivery are analyzed to determine the optimal configuration for each fuel and strategy. During analysis, different injection locations are explored, such as port fuel injection and direct injection, as well as injection timing, and other injection parameters. Performance metrics such as cylinder mixing and fuel impingement on engine surfaces are evaluated, with the goal of maximizing mixing homogeneity and combustion efficiency. While these simulations are on a small displacement diesel engine, the results apply to larger diesel engines.

This work shows the viability of ammonia and methanol as alternatives or partial substitutes for traditional carbon-based fuels by demonstrating the potential of optimized combustion strategies for existing diesel architecture using non-carbon and carbon neutral fuels, which represents an important step toward global decarbonization.

1 INTRODUCTION

Across industry there is a widespread push to reduce Greenhouse gas (GHG) emissions. For example, the International Maritime Organization's (IMO) 2023 resolution targets a GHG reduction of 20% by 2030 and 70% by 2040. This initiative along with many others is motivating the large engine market to pursue more efficient power with lower GHG emissions through the development of advanced technology and alternative fuels.

Two fuels that have been proposed as potential carbon neutral or low carbon substitutes are ammonia and methanol [1]. Dual-fuel diesel engine operation with methanol or ammonia presents a carbon emissions reduction opportunity with minimal modification to the base diesel system. This includes maintaining the diesel systems high compression ratio and having diesel back-up capability, enabling dual-fuel operation and conventional diesel combustion (CDC) without sacrificing the base diesel system performance.

Woodward is working with a number of OEMs on methanol and ammonia dual-fuel engines, who are conducting experimental programs and sharing qualitative results with us. From this experience, we have seen several common issues. The purpose of this paper is to demonstrate the use of Computational Fluid Dynamics (CFD) to help others pursuing alternative dual-fuel technologies avoid these same challenges.

This paper details the use of CFD to address common problem areas and detail system modifications required to match and exceed the existing diesel systems performance with an aggressive secondary fuel substitution rate of 90% by energy. The main areas of focus will be injection strategy and timing, required injector placement, manifold conditions and equivalence ratio.

2 COMBUSTION BASELINE AND TARGETS

Analysis was performed using the cylinder geometry of a 6.8L agricultural diesel engine, geometric parameters detailed in Table 1. For this research, the engine's performance is analyzed at 1500RPM with a target indicated mean effective pressure (IMEP) of 22bar.

Converge CFD was used to model the combustion performance of the single cylinder geometry detailed in Table 1. The base CDC operating parameters to achieve an IMEP of 22bar at 1500RPM are detailed in Table 2. The combustion mechanism and base model were supplied by John Deere. Slight variations were made to approximate the implementation of Woodward products designed to improve pumping work and EGR addition. The kinetic mechanism for dual-fuel combustion of diesel and ammonia is taken from *A Skeletal Chemical Kinetic Mechanism for Ammonia n-Heptane combustion* [2]. The kinetic mechanism for dual-fuel combustion of diesel and methanol is taken from *A New Skeletal Chemical Kinetic Mechanism for Methanol n-Heptane Dual-fuel* [3]. In both dual-fuel mechanisms n-Heptane is used as a surrogate for diesel. The base diesel modeling for diesel spray and combustion were validated in previous programs, [4,5,6], giving us confidence in their use here. There are also a number of studies in the area of ammonia and ammonia-diesel dual-fuel [1,7,8,9,10].

Table 1. Engine geometric parameters

Parameter	Value	Units
Bore	106.5	mm
Stroke	127.0	mm
Connecting Rod Length	221.7	mm
Geometric Compression Ratio	16.8	
Effective Compression Ratio	16.3	

Table 2. Base diesel configuration at 1500RPM

Parameter	Value	Units
Intake Manifold Air Pressure	355.1	kPa
Manifold Air Temperature	335.2	Kelvin
Exhaust Manifold Pressure	374.0	kPa
Air mass per cycle	3602.7	mg
Diesel mass per cycle	125.6	mg
Diesel Start of Injection	-5	CA ATDC
Diesel Injection Duration	24	CA
Injection Pressure	1837	bar
Lambda	1.5	
EGR Rate[1]	22.0	%

[1]Diesel Definition of EGR

The model was run using the SAGE detailed chemistry solver. Liquid injection of methanol and diesel were modeled using a Eulerian-Lagrangian approach to simulate droplet introduction, breakup and evaporation. The same Eulerian-Lagrangian approach is used to simulate spray wall impingement, film accumulation and film separation back into air flow. The CFD model geometry is shown in Figure 1.

The simulated cylinder pressure trace and apparent heat release rate (AHRR) of the CDC system described above is shown in Figure 2 with combustion metrics listed in Table 3. The performance of the unmodified diesel system will be used as the baseline for the performance of the ammonia and methanol dual-fuel configurations. To match the combustion performance of the CDC system the combustion strategy for both dual-fuel combinations will target Center-Of-Combustion, CA50, of 12.5CA ATDC with a burn duration of 15CA, while not exceeding a peak pressure of 200bar and a pressure rise rate of 10 bar/CA.

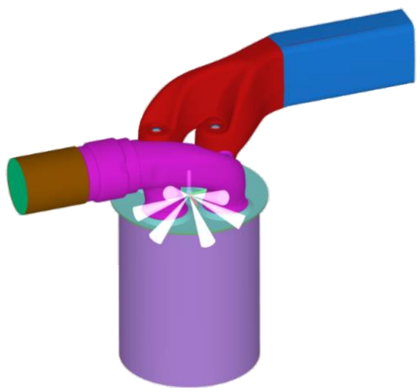

Figure 1. Converge Model Setup

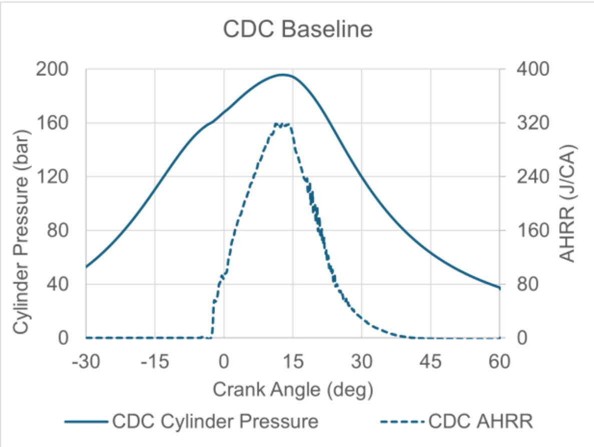

Figure 2. Base diesel 22bar IMEP pressure trace and heat release simulation

Table 3. Base diesel performance metrics

Parameter	Value	Units
Peak Pressure	195.7	bar
Peak Pressure Angle	12.8	CA
Peak Pressure Rise Rate	5.0	Bar/CA
CA10	3.2	CA
CA50	12.4	CA
CA90	22.3	CA
Burn duration	19.1	CA
Diesel mass per cycle	125.6	mg

Since for any given CFD run, the start of combustion cannot be known a'priori, Figure 3 shows the relationship between the resultant CA50 and burn durations to indicated efficiency. The lower limit of CA50 for each burn duration curve was chosen to minimize heat release before top dead center (TDC). The CDC baseline is marked on the graph along with the target dual-fuel performance.

The alternative fuel rate for a target 90% substitution by energy is noted in Table 4 along with the differences between the three fuels. Methanol and ammonia have similar energy content per unit mass which is a little under half of diesel's energy content. To achieve 90% fuel substitution by energy the fuel mass will need to roughly double relative to the diesel mass for the base case shown in Table 2.

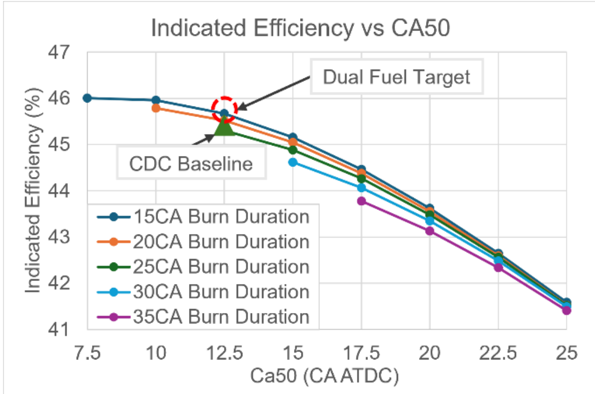

Figure 3. Relationship between indicated efficiency and CA50 with varied burn durations

Table 4. Comparison of the three fueling cases

Fuel	Lower Heating Value (MJ/kg)	Air Fuel Ratio	Fuel Mass for 90% Energy Substitution Rate (mg/cycle)
Diesel[1]	43.25	15.1	12.9
Methanol	19.9	6.4	253.1
Ammonia	18.6	6.1	270.8

[1]Approximated as C_7H_{16} for combustion simulation

The initial analysis utilizes a simplified cylinder model, shown in Figure 4, to optimize the combustion recipe for the two dual-fuel configurations. The components removed from the full model to create the simplified model include the valve opening and closing events, evaporation of fuel droplets and mixing of gaseous fuel.

The simplified model imposes cylinder pressure, temperature, and a homogeneous gaseous composition at the point of intake valve closure. By eliminating valve-opening and valve-closing events and assuming a fully mixed gaseous composition combustion can be simulated in approximately one-eighth the time required by the full model. This streamlined approach is depicted in Figure 4. Following the refinement of the combustion strategy using the simplified model, the full cylinder model will be updated to replicate the cylinder conditions determined by the simplified model.

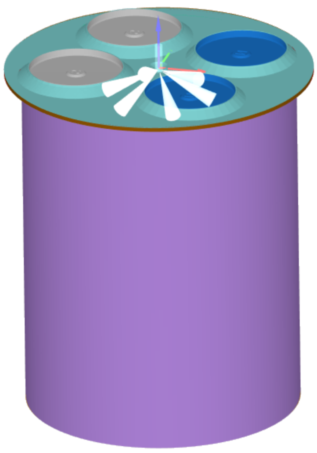

Figure 4. Simplified Cylinder Converge Model

3 METHANOL-DIESEL DUAL-FUEL MODELING

When the motored pressure, EGR and fuel energy are approximately matched to the CDC baseline in the methanol-diesel simple cylinder model, as detailed in Table 5, rapid combustion is observed as shown in Figure 5.

Table 5. Base methanol CDF configuration parameters at 1500RPM

Parameter	Value	Units
Intake Manifold Air Pressure	371.4	kPa
Intake Manifold Air Temperature	335.2	Kelvin
Air mass per cycle	3850.9	mg
Diesel mass per cycle	12.9	mg
Methanol mass per cycle	253.1	mg
Diesel Start of Injection	-5	CA ATDC
Diesel Injection Duration	3.78	CA
Injection Pressure	2000	bar
Lambda	1.6	
EGR Rate[1]	22.0	%

[1]Diesel Definition of EGR

The methanol dual-fuel case exhibits a slightly earlier center of combustion and a much shorter burn duration than the diesel base case, noted in Table 6. These two factors lead to an unacceptably rapid pressure rise and a peak cylinder pressure of 367bar which far exceeds the maximum allowable cylinder pressure. This model assumes that all methanol enters the cylinder as a vapor, no energy is lost from the charge air during this process and that the cylinder is a perfectly homogeneous quiescent mixture at intake valve close (IVC).

To address the unacceptable pressure rise and peak pressure, the simple cylinder model is used to determine combustion strategy modifications. In a separate analysis, the intake manifold is resolved and the injection strategy impact on fueling, mixing and evaporative cooling will be analyzed during intake and compression.

Table 6. Comparison of diesel to methanol dual-fuel combustion with similar combustion strategy

Fuel	CA50 (deg)	Burn Duration (deg)	Total Heat Release (Joules)
Diesel	12.4	19.1	5435
Diesel-Methanol	2.2	2.3	5491

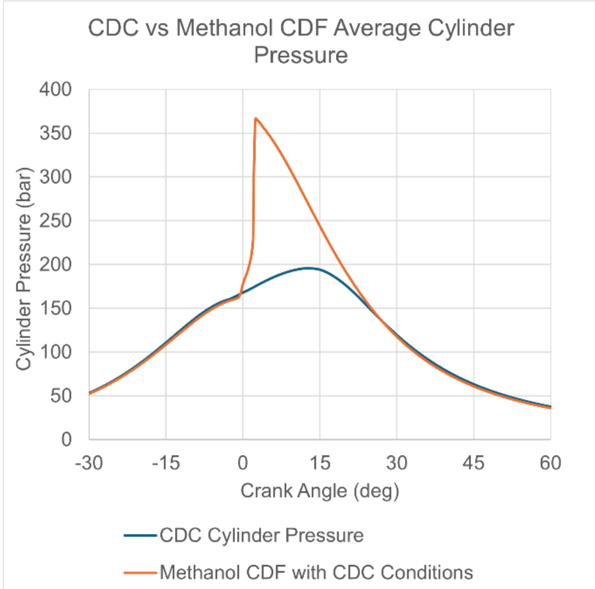

Figure 5. Cylinder pressure comparison of CDC and methanol CDF at similar operating point

3.1 Combustion investigation

Using the simplified cylinder model a sweep of cylinder temperature at IVC was done to determine the impact of lowering the manifold air temperature (MAT) and leveraging the evaporative cooling effect of methanol. The difference in latent heat of vaporization between the diesel surrogate - heptane, and methanol are shown in Table 7. The extra methanol mass further enhances its cooling potential.

Table 7. Comparison of n-heptane fluid properties to methanol

Fuel	Latent Heat of Vaporization (kJ/kg)	Boiling Point at 1 atm (Kelvin)
Heptane	318	371.5
Methanol	1100	337.9

The pressure traces in Figure 6 show the effect of the trapped in-cylinder temperature at IVC. Lowering the effective MAT by 30°C, from 62°C to 32°C, slows the burn duration from 2.3CA to 9.8CA as shown in Table 8. This change in the speed of combustion lowers the peak cylinder pressure from 367bar to 255bar.

Table 8. Comparison of methanol dual-fuel combustion with varied manifold air temperature

Manifold Air Temperature (°C)	CA50 (deg)	Burn Duration (deg)	Total Heat Release (Joules)
62	2.2	2.3	5491
52	4.6	3.9	5481
42	7.3	8.2	5468
32	10.4	9.8	5465

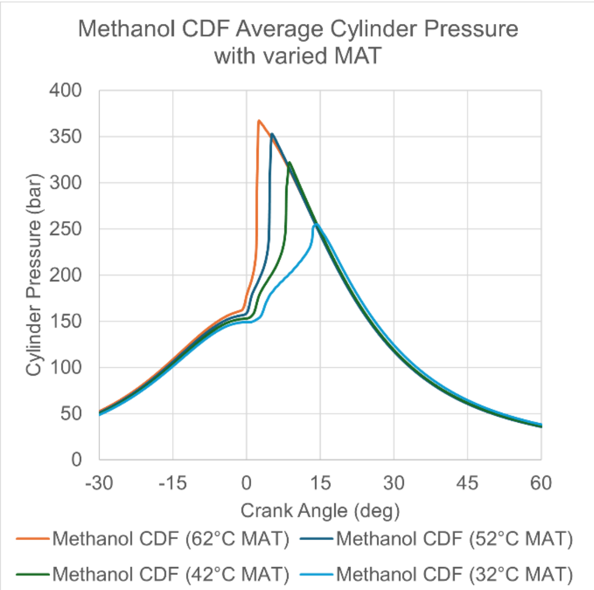

Figure 6. Effect of charge temperature on combustion rate

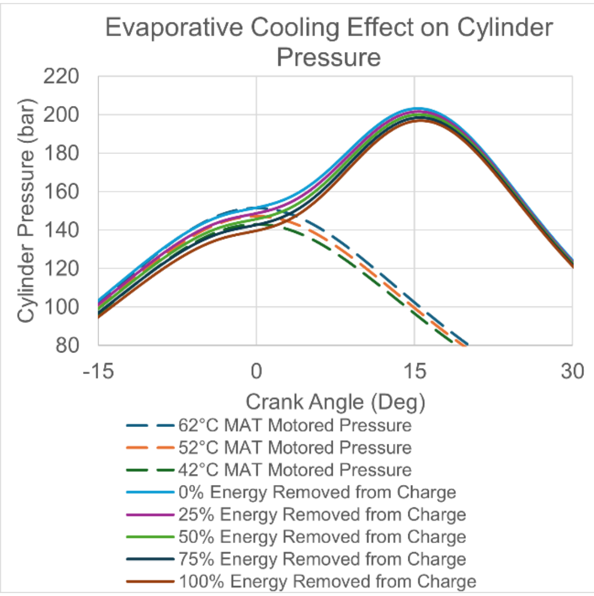

Figure 7. Effect of evaporative cooling on cylinder pressure

Evaporative cooling plays an important role as well. The amount of energy removed from the charge lowers the motored cylinder pressure before the diesel injection event as expected. Figure 7 shows the combustion changes as well. For example, if the energy required to evaporate 25% of the injected methanol is pulled from the charge after IVC the resulting change in motored pressure is equivalent to a reduction in the charge air temperature of 10°C. This removal of energy from the charge also results in a slight reduction in work during compression. Another benefit of the methanol evaporative cooling during intake is an effective increase in volumetric efficiency [11].

During methanol-diesel Conventional Dual-fuel (CDF) combustion, it is observed that the diesel spray plumes impinge on the piston bowl where the liquid mass begins to evaporate. This leads to the vaporized diesel being located toward the outer edge of the piston causing combustion to begin at the outer edge of the bowl. As combustion progresses, the flame front moves inward towards the center of the piston bowl as seen in Figure 8. This “outward-in” combustion concentrates the diesel-methanol mixture into the center of the piston bowl where once ignited releases the remaining fuel energy rapidly. This rapid release of energy can be seen in the heat release profiles shown in Figure 9 where a spike in the heat release rate is evident near end of combustion.

To slow the rapid heat release at the end of combustion the diesel injection event is split into two pulses. Splitting the diesel injection event allows for the first pulse to impinge on the piston and begin evaporating. As combustion begins at the edge of the piston bowl a second injection event occurs adding diesel into the unburnt region at the center of the piston bowl. As the flame front from the first injection event begins to move inward, the diesel from the second injection event begins to evaporate and burn in a diffusion flame as shown in Figure 10. This, in conjunction with the slower flame propagation at the edge of the piston due to the reduced amount of diesel that impinges on the piston bowl, leads to slower heat release as shown in Figure 11. By tuning the first injection event to control the timing of CA10 and the second injection event to control the burn duration the split injection strategy allows for control of combustion phasing and timing.

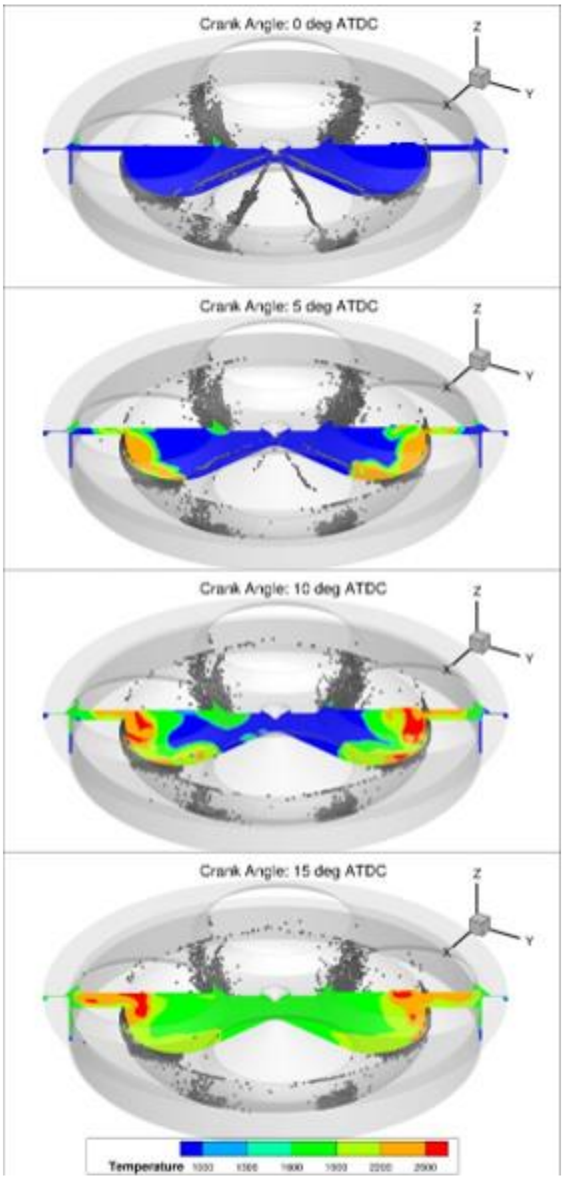

Figure 8. Evolution of temperature fields for the methanol 32°C CDF combustion showing the inward collapse of combustion

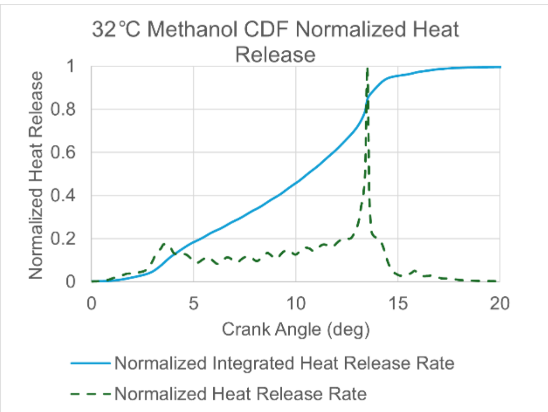

Figure 9. Normalized integrated heat release of 32°C charge methanol CDF showing rapid heat release at end of combustion

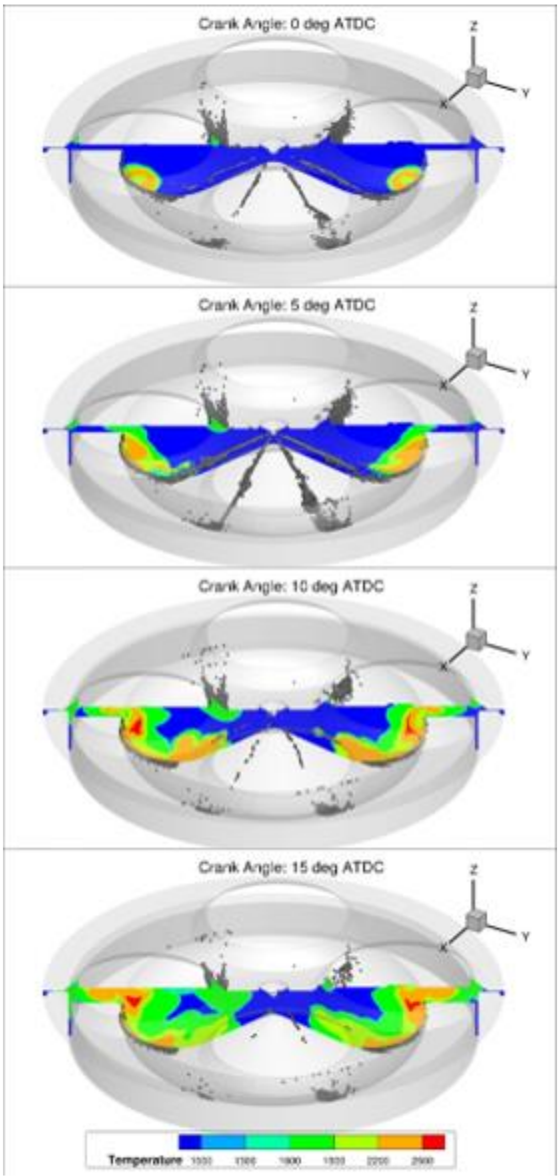

Figure 10. Evolution of temperature fields for the methanol 32°C CDF combustion with split diesel injection event dSOI at -7 and 2CA

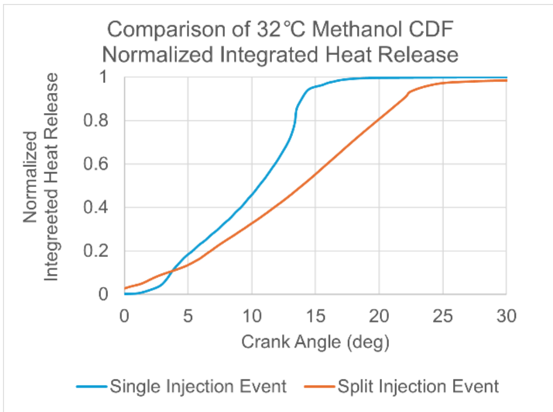

Figure 11. Comparison of methanol CDF combustion normalized integrated heat release with and without split injection event

3.2 Methanol Injection Analysis

From the coarse combustion recipe development using the simple model, a methanol injection strategy needs to be determined to produce the homogenous, fully-evaporated environment in cylinder before the diesel start of injection. The two fuel injection strategies that will be explored for methanol fuel introduction are Port Fuel injection (PFI) and Direct Fuel injection (DI). Due to the high latent heat of vaporization and lower energy content per unit mass of methanol, compared to diesel, methanol poses a risk of accumulating as a film on the liner and piston rather than being evaporated into the air EGR mixture. Figure 12 shows the three injection locations that will be explored, two PFI locations and one DI location. The DI installation location was chosen to coincide with the installation location of a glow plug in the base diesel configuration. This decision was made to minimize the complexity of retrofit to the base diesel head. The two PFI installation locations shown are spaced at 50mm intervals from the first intake valve.

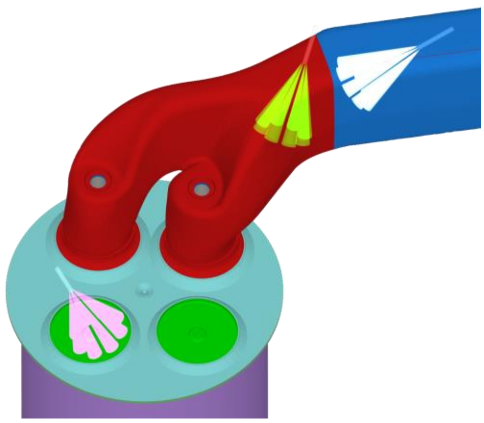

Figure 12. Illustration of different installation points for methanol Injectors

To maximize mixing and minimize wall wetting with both PFI and DI strategies, the injection timing must be carefully phased to complement the air flow and piston position. For PFI configurations, injection timing is heavily dependent on the intake and exhaust valve timing. In this engine configuration, there is back-flow from the cylinder into the intake during the period of intake and exhaust valve overlap. For ideal performance, injection during this backflow period should be avoided. Injection should begin only once the air is flowing into the cylinder and terminated while there is still sufficient air flow to carry the last of the injected mass into the cylinder.

The relative distance of the port fuel injector to the intake valves also affects end of injection as the last of the injected mass must have time to travel into the cylinder before the intake valve closes. These factors significantly restrict the start and end of injection. As can be seen in Figure 13, the PFI injection duration is limited to 90-130CA due to the air flow in the intake. For the sake of this analysis the duration of injection is limited to 90CA to accommodate the different injector placement locations and to provide additional time for the air flow to strip any liquid film from the wall.

Wall Wetting. From a wall wetting perspective, the direct injection configuration is less dependent on the valves position since the fuel is introduced directly into the cylinder. To minimize in-cylinder wall wetting, the position of the piston is of more importance. When the methanol is injected after Bottom Dead Center (BDC) there is an increased risk of unevaporated methanol droplets impinging on the piston and forming a film. For an effective methanol DI strategy wall wetting and evaporative cooling as well as vapor mixing need to be balanced. This balancing act leads to an ideal injection duration between 90-180CA. From independent spray simulations, it was found that 160CA injection duration with a start of injection (SOI) of -300CA ATDC provided the necessary cooling to the charge while minimizing film accumulated on the piston.

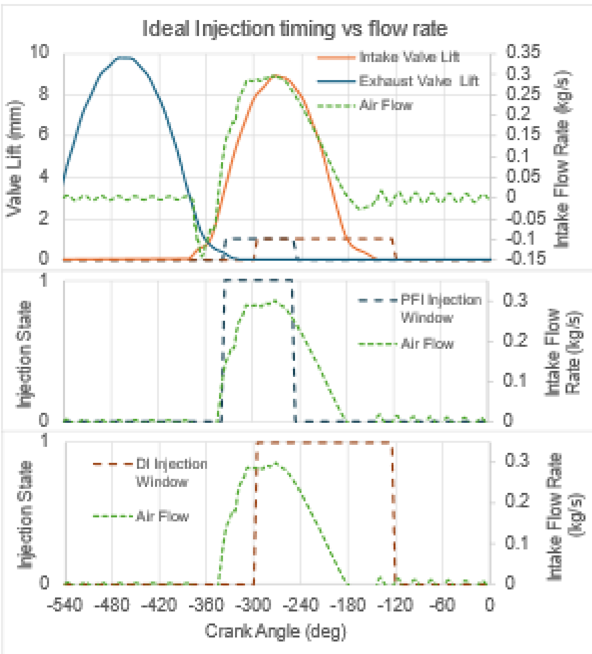

Figure 13. Ideal injection timing for DI and PFI system given valve timing and air flow

Fuel Injection Pressure and Spray. As noted by Willmann, et. al, purpose-built methanol applications leverage high pressure dual-fuel systems but retrofits and newbuilds are limited to lower pressure, traditionally, PFI systems [12]. For this analysis a fuel supply pressure of 200bar will be assumed for both injection strategies as this is the uppermost pressure any OEM worked with has consider for retrofit. The design of the injector plays a large part in the resulting atomization of the spray and needs to be adapted to each application. For the purposes of this analysis where determining the ideal placement is the primary goal, similar injector parameters leveraging eight spray holes of equal size will be assumed for both the PFI and DI case but with slight adjustment to the spray hole diameters to allow for the ideal injection window described above to be implemented, shown in Table 9.

Table 9. Injector parameters for each injection strategy

	Injection Duration (CA)	Start of Injection (CA ATDC)	Spray Hole Diameter (mm)
PFI (100mm)	90	-335	0.175
PFI (50mm)	90	-335	0.175
DI	160	-300	0.132

PFI is desirable due to the ability to retrofit existing engines with minimal or no modifications to the head. Ideally the injector could be installed in the intake manifold and aimed in the direction of the air flow, but this causes large amounts of wall wetting due to the droplets impinging on the wall near the intake valves. Injected mass that is accumulated as film will eventually be evaporated and burned but could lead to evaporated fuel being ingested by an adjacent cylinder leading to cylinder-to-cylinder variation or a time delayed evaporation of fuel leading to degradation of transient response. Research done by SWRI investigating injection requirements for methanol cold-start concluded that in a system with no “pre-vaporization”, no energy pulled from engine walls, a droplet size of 10µm was required for the droplets to be entrained in the air flow and enter the cylinder without impinging on the wall or valve seat [11].

In all simulations run with the injector parameters described in Table 9, the average Sauter Mean Diameter predicted during injection by the CFD simulation exceed the 10µm requirement which leads to the droplets impinging on surfaces in the vicinity of the injection site. This is worst for the PFI case positioned 100mm from the valve which shows significant film accumulation as shown in Figure 14. This leads to large quantities of the injected methanol being trapped in the intake runner at IVC. The distribution and state of the injected methanol is detailed in Table 10.

Table 10. Fuel distribution with PFI positioned 100mm from intake Valve at IVC (-150CA ATDC)

	Droplet Mass (mg)	Vapor Mass (mg)	Film Mass (mg)
Intake	0	0.3	133.3
Cylinder	8.0	111.0	0.5

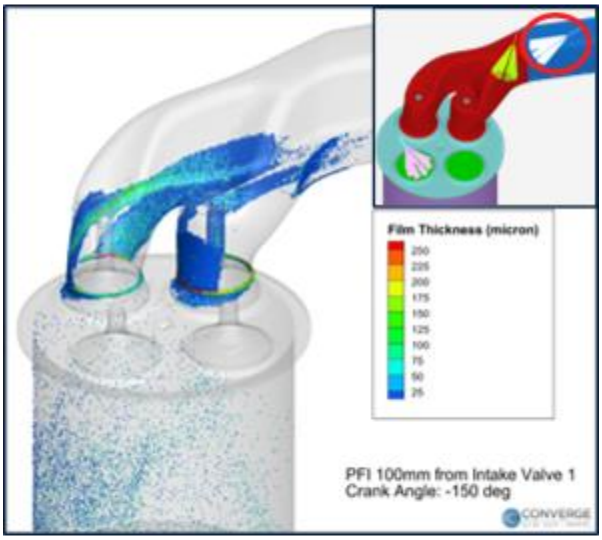

Figure 14. Wall film produced during a single injection event with a PFI 100mm from intake valve

A potential solution to these draw backs of PFI is to position the injector targeting one of the intake valves. This placement significantly reduces the risk of intake manifold wall wetting due to the proximity of the injection to the cylinder. Evaporation is further improved by the proximity of the hot intake valve, which provides energy to evaporate the liquid fuel. The reduced wall film thickness at IVC is shown in Figure 15 along with the distribution of the injected methanol in Table 11.

Table 11. Fuel distribution with PFI positioned 50mm from Intake valve at IVC (-150CA ATDC)

	Droplet Mass (mg)	Vapor Mass (mg)	Film Mass (mg)
Intake	0.0	0	64.3
Cylinder	24.0	153.5	3.6

This strategy can be further improved by installing the injector further into the intake runner to isolate the spray from the airflow before the intake runner splits leading to the intake valves. This prevents the spray from impinging on the wall where the intake runner splits and allows for the spray plumes to be directed at the back of a single intake valve. This can also be done by extending the injector into the intake runner to reduce the distance between the tip of the injector and the intake valve. However, both these strategies may increase the complexity of the engine modification.

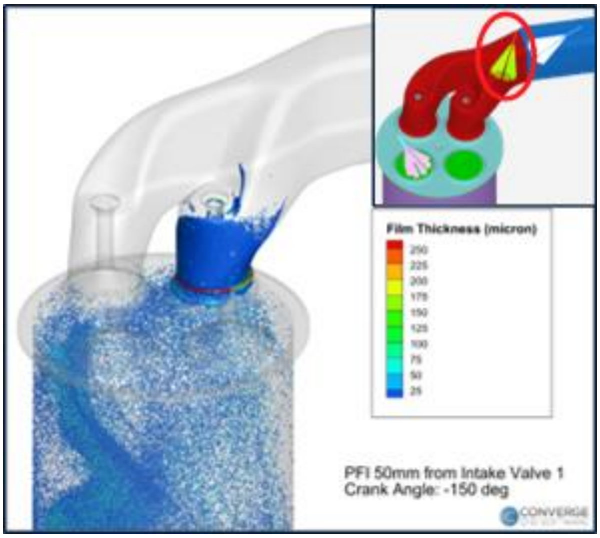

Figure 15. Methanol wall film with PFI positioned 50mm from Intake valve at IVC (-150CA ATDC)

DI Strategy. In addition to avoiding possible transient and cylinder to cylinder variation caused by excess wall wetting from a PFI strategy, DI injection strategy leverages the high latent heat of vaporization as discussed above. This is due to the energy used to evaporate the methanol coming from the charge rather than from a wall. To properly leverage the cooling effect the injector needs to produce droplet that evaporate before impinging on an engine surface. In the cylinder, the liner and piston are sufficiently warm to evaporate small amounts of methanol film but the energy for evaporation is pulled from the wall rather than from the charge. Implementing the injection strategy described above with nozzle orifice size described in Table 9, the DI case pulls approximately 20% of the energy for evaporation from the charge after IVC as shown in Figure 16.

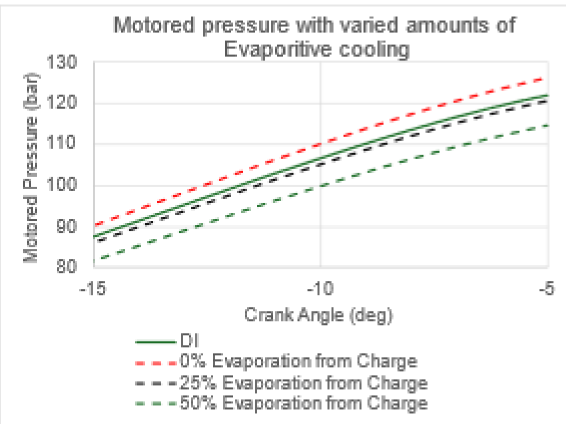

Figure 16. DI Injection strategy evaporative cooling effect on motored pressure trace compared to amount of available energy

3.3 Methanol Results

In modeling the full cylinder, it was found that the simple model underpredicted the reactivity of the charge leading to higher cylinder pressures than initially predicted by the simple model. Potential sources for this discrepancy in reactivity could be attributed to the non-homogenous fuel distribution, trapped hot residuals and radicals from previous cycles. To compensate for the increased reactivity observed in the full model, the lambda was lowered to 1.3 and the EGR rate was increased to 25%. With these two alterations to the simple model configuration, a combustion strategy targeting an inlet temperature of 40°C, a DI methanol injection strategy and a split injection event, as detailed in Table 12, was analyzed.

Table 12. Optimized methanol CDF configuration parameters at 1500RPM

Parameter	Value	Units
Intake Manifold Air Pressure	294.7	kPa
Manifold Air Temperature	313.2	Kelvin
Exhaust Manifold Air Pressure	305.6	kPa
Diesel mass per cycle	6.45/6.45	mg
Diesel Start of Injection	-5/4	CA ATDC
Diesel Injection Duration	1.78/1.78	CA
Injection Pressure	2050	bar
Methanol mass per cycle	253.1	mg
Methanol Start of Injection	-300	CA ATDC
Methanol Injection Duration	160	CA
Lambda[1]	1.3	
EGR Rate[2]	25.0	%

[1]Diesel Definition of EGR

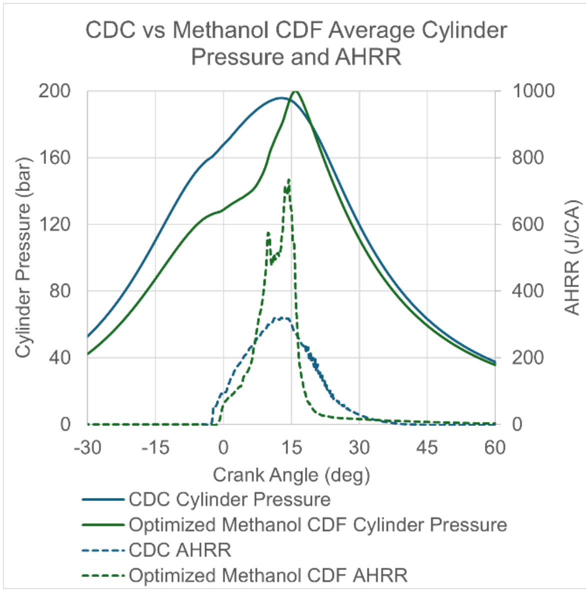

Figure 17. Cylinder pressure comparison of CDC and optimized methanol CDF

These modifications to the findings of the simple methanol-diesel CDF case resulted in an acceptable peak pressure of 200bar and peak pressure rise of 10bar/CA in the full cylinder model. A comparison of the cylinder pressure traces and apparent heat release rate from the optimized methanol system to the CDC base configuration can be seen in Figure 17. As noted in Table 13, the optimized methanol case has a more aggressive CA50 and burn duration than the base diesel, which would suggest delaying diesel injection timing to lower peak pressure and pressure rise to add operating margin for methanol.

Table 13.Optimized Methanol CDF Performance

Parameter	Value	Units
Peak Pressure	200.0	bar
Peak Pressure Angle	15.9	CA
Peak Pressure Rise Rate	10.0	bar/CA
CA10	5.8	CA
CA50	12.4	CA
CA90	17.6	CA
Burn duration	11.8	CA

4 AMMONIA-DIESEL DUAL-FUEL MODELING

Combustion results for an ammonia-diesel CDF system at the 90% substitution rate when using a traditional CDF combustion strategy with similar boundaries as the CDC baseline, as detailed in Table 14, can be seen in Table 15. In the ammonia case the injected diesel evaporates and burns quickly but as the flame propagates it is quickly quenched by the ammonia mixture as shown in Figure 19. This leads to a combustion efficiency less than 50%. In short, in CDF, the ammonia burns in the "Halo" of the diesel, but not well on its own.

Table 14. Base ammonia CDF configuration parameters at 1500RPM

Parameter	Value	Units
Intake Manifold Air Pressure	367.0	kPa
Intake Manifold Air Temperature	335.2	Kelvin
Air mass per cycle	3565.2	mg
Diesel mass per cycle	12.9	mg
Ammonia mass per cycle	270.8	mg
Diesel Start of Injection	-5	CA ATDC
Diesel Injection Duration	3.78	CA
Injection Pressure	2000	bar
Lambda	1.6	
EGR Rate[1]	22.0	%

[1]Diesel Definition of EGR

Table 15. Comparison of the base diesel to ammonia dual-fuel

Fuel	CA50 (deg)	Burn Duration (deg)	Total Heat Release (Joules)
Diesel	12.4	19.1	5435
Diesel-Ammonia	-[1]	-[1]	2415

[1]Only half of fuel energy was released in CDF Ammonia case

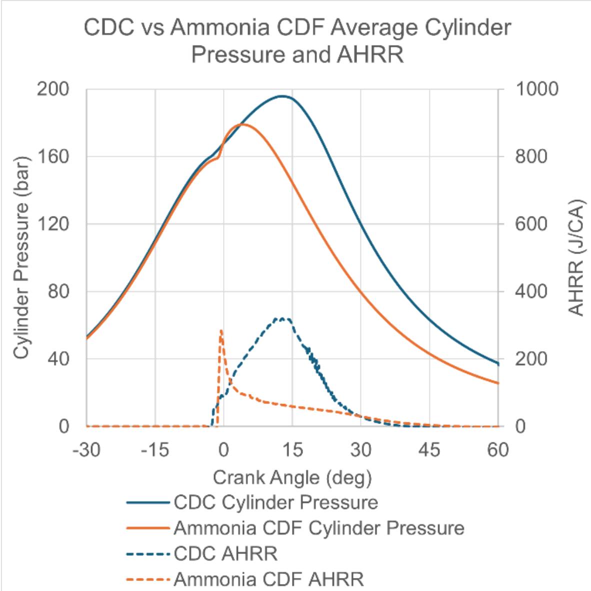

Figure 18. Cylinder pressure and apparent heat release rate comparison at similar operating point

It was found by Chiera, et. al [4,5,6], that CDF combustion works well for a reactive fuel like natural gas, where once the ignition is initiated by the diesel pilot injection, the flame could propagate in the air-substitution fuel mixture, but there were still flame speed limitations. To address the limitations of CDF, Reactivity Controlled Compression Ignition (RCCI) combustion was demonstrated on both natural-gas-diesel dual-fuel and ammonia-diesel fuel. In these RCCI studies, the heat release rate at high substitution rates exceeded that of the base diesel combustion, resulting in higher indicated efficiency and much lower fuel slip. In RCCI combustion, two fuels with widely disparate reactivity are used making ammonia an ideal second fuel for RCCI diesel combustion. To improve the heat release rate in the ammonia case a combustion strategy leveraging RCCI is investigated.

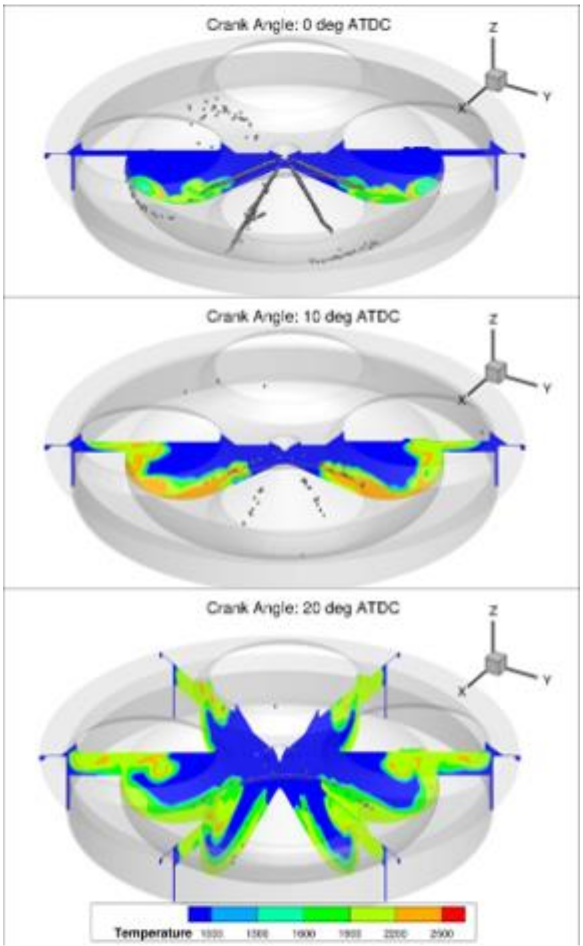

Figure 19. Evolution of Temperature Fields for Ammonia CDF Combustion

4.1 Ammonia Combustion Analysis

To achieve RCCI combustion with the ammonia-diesel system the reactivity must be increased. Using the simple cylinder model the effects of removing EGR, increasing cylinder temperature and decreasing lambda were analyzed. Leveraging the findings of Chiera, et. al, an early diesel start of injection (SOI) of -40CA ATDC was used in the RCCI Cases [4]. A comparison of the normalized integrated heat release can be seen in Figure 20.

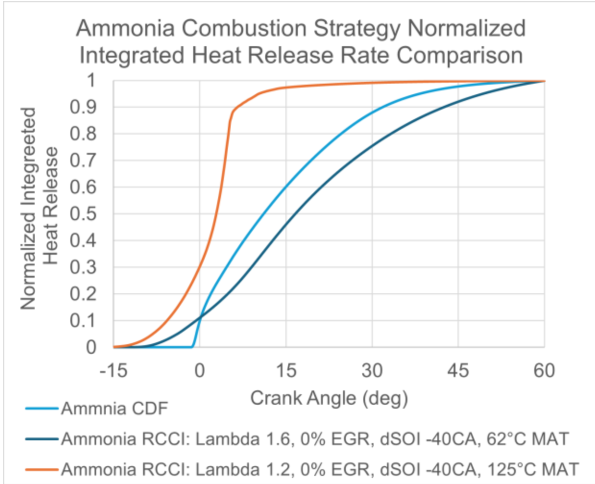

Figure 20. Comparison of normalized heat release rate with varied cylinder conditions and combustion strategy

The higher reactivity RCCI cases showed more rapid heat release than the baseline case but suffered from a large amount of energy being released before TDC. To delay CA10, the timing of the diesel injection event during compression was advanced to -60CA ATDC. As noted by Chiera, et. al, advancing injection timing delays ignition in RCCI combustion due to the earlier injection providing more time for the diesel vapor to mix with the charge which lowers the local AFR [4].

Split-Injection RCCI. As seen in the normalized integrated heat release in Figure 21, splitting the diesel injection event into two equal events and advancing the timing of the first event shows improved heat release and a more favorable CA10.

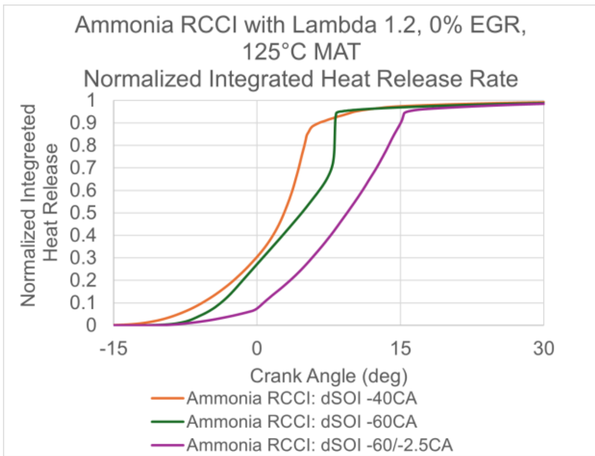

Figure 21. Comparison of normalized heat release rate implementing RCCI combustion with Lambda 1.2, 0% EGR and 125°C MAT with varied diesel injection strategy

4.2 Ammonia Dual-fuel Mixing Analysis

Due to the vapor pressure of ammonia being near 10 bar at room temperature, Port Fuel Injection is the only strategy simulated for gaseous anhydrous ammonia. A Woodward Solenoid Operated Gas Admission Valve (SOGAV), example shown in Figure 22, is assumed for fuel introduction into the intake runner. This is done through the addition of a feed pipe into the intake runner where the gas is fed by the SOGAV. From the CDC base configurations, Table 2, and the required fuel mass, Table 4, a SOGAV11 flow characteristics were imposed at the pipe inlet.

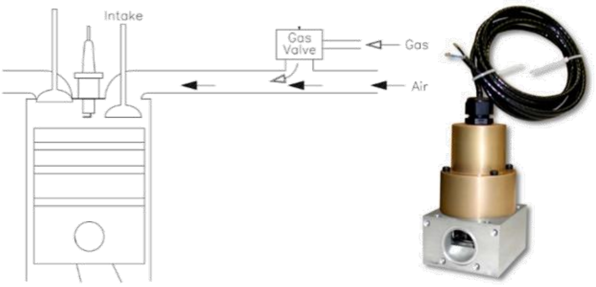

Figure 22. SOGAV manual installation guide illustration

The diameter of the post SOGAV feedpipe was sized to match the effective area of the SOGAV to prevent a delay in the transport of ammonia into the intake runner. If the piping after the SOGAV, or any other gaseous port fuel injector, is smaller than the effective area of the injector the fuel will experience a transport delay, increasing the risk of the fuel being left in the intake runner and manifold. Any fuel that is not ingested by the target cylinder could be consumed by an adjacent cylinder.

Like the methanol PFI cases previously discussed, the ideal timing for ammonia introduction is after the intake valve is open, the exhaust valve is closed, and there is positive flow into the cylinder. This minimizes short-circuiting, backflow and improves fuel-air mixing. Further, matching the fuel flow rate to the air flow rate, the instantaneous composition enters the cylinder near the target average lambda as seen in Figure 23.

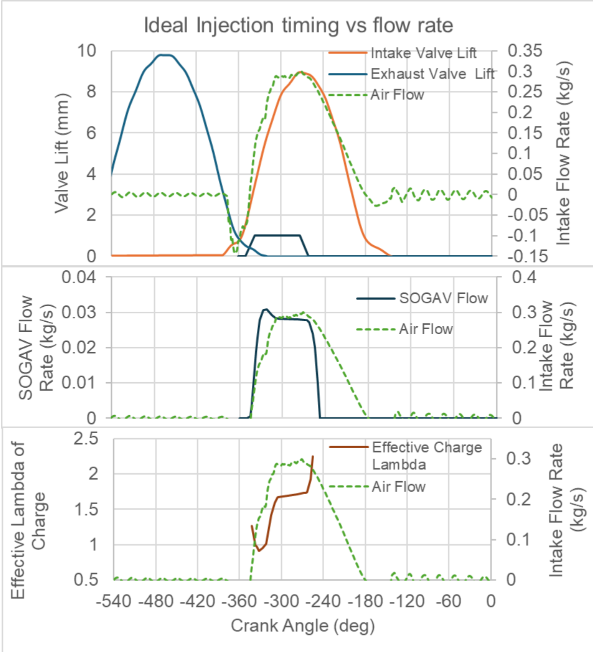

Figure 23. SOGAV injection timing relative to intake valve opening to optimize fuel delivery

To optimize fuel delivery to the cylinder several feed pipe placements and lengths were analyzed, Figure 24. The coefficient of variation (COV) was used to evaluate in-cylinder mixing uniformity. The ideal target for uniformity would be a COV of 0%. Defining a peak acceptable COV of lambda exceeds the scope of this paper and work is instead focused on minimizing the value. It was found that the composition near TDC in all cases were similar in uniformity except for the pipe that entered the intake manifold 100mm from the first intake valve and ran 75mm into the intake runner, shown in Figure 25.

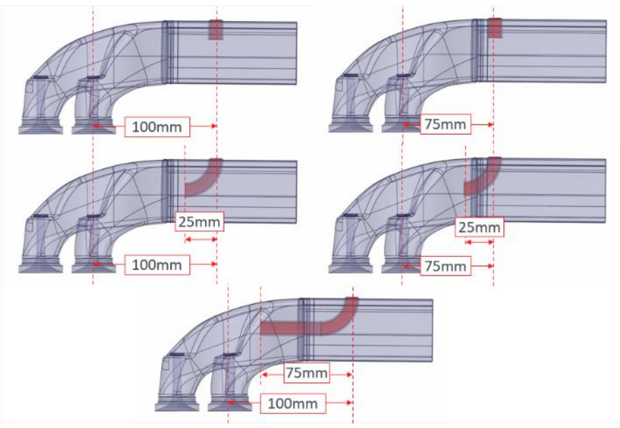

Figure 24. Simulated Ammonia Feed Pipe Configurations

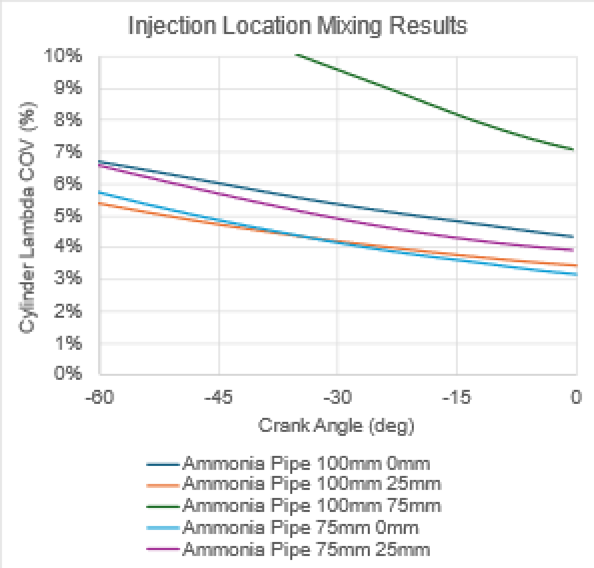

Figure 25. Lambda coefficient of variation near TDC with varied ammonia feedpipe length and location

As can be seen in Figure 26, a small amount of mass is lost from the cylinder during compression due to late intake valve close but the lost mass only accounts for ~1% of the total injected fuel mass. All feed pipe configurations have similar in cylinder trapped fuel mass apart from the 75mm pipe in the intake runner which had 2-3% less of the injected fuel in cylinder at intake valve close. The lower amount of trapped mass in this case can be attributed to the extra length of the feed pipe which is not completely evacuated before IVC which results in ~5% of injected mass being trapped in the intake runner.

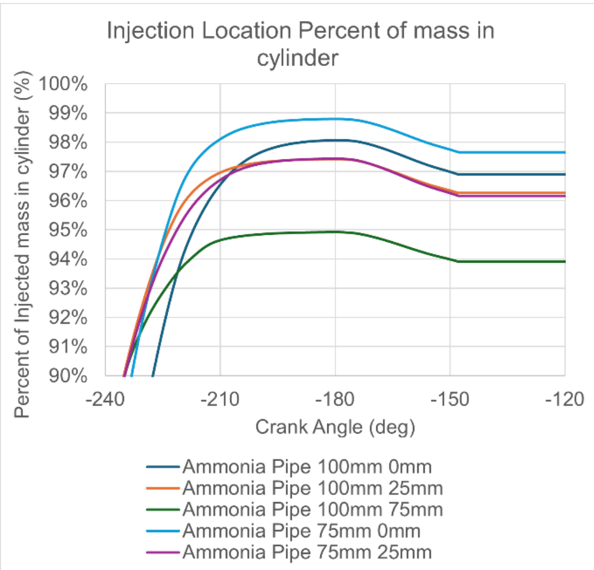

Figure 26. Fuel mass in cylinder near IVC with varied feed pipe configurations

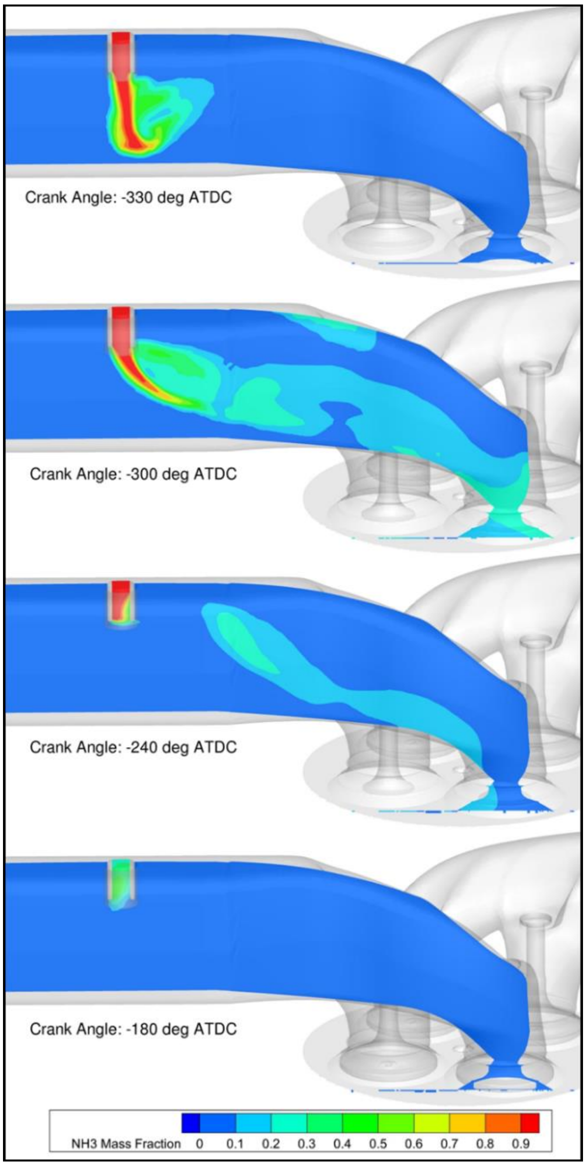

Figure 27. Contour of ammonia mass fraction during an injection event

From this analysis it was determined the short vertical feed pipe 100mm from the first intake valve provided the best performance. This configuration showed the lowest fuel mass lost to the intake while minimizing the in-cylinder lambda coefficient of variation. The short feed pipe reduces the volume where ammonia can be trapped after the end of injection as well as introducing the gaseous fuel into cross flow which effectively mixes the charge when injected with the ideal timing shown in Figure 23. Figure 27 shows a cross-section of the intake runner with ammonia mass fraction during an injection event mixing and entering the cylinder.

4.3 Ammonia results

Leveraging a RCCI combustion strategy with the lessons learned from on-engine testing at Woodward [4] and the simple combustion model, the full cylinder model with split injection, as detailed in Table 16, enabled complete combustion of the fuel mixture. To achieve the increase in cylinder temperature found in the simple model the MAT was increased to 80°C and the exhaust back pressure was held at 406kPa to increase hot residuals trapped in cylinder at exhaust valve close. A comparison of the average cylinder pressure traces and apparent heat release rate from the optimized ammonia RCCI system to the CDC base configuration can be seen in Figure 28. The optimized RCCI ammonia system achieves an acceptable peak pressure of 194.1bar and peak pressure rise of 5.6bar/CA. The system also met the target CA50 and burn duration targets as shown in Table 17.

As noted in the methanol CDF results, the simple ammonia-diesel cylinder model underpredicted the reactivity of the charge which can be attributed to the same factors listed in the methanol results. To account for this, the second diesel injection event in the RCCI split injection event strategy was delayed 1.5CA compared to the split injection case in Figure 21.

Table 16. Optimized Ammonia CDF at 1500RPM

Parameter	Value	Units
Intake Manifold Air Pressure	296.3	kPa
Intake Manifold Air Temperature	353.15	Kelvin
Exhaust Manifold Air Pressure	406.0	kPa
Diesel mass per cycle	6.45/6.45	mg
Diesel Start of Injection	-60/-1	CA ATDC
Diesel Injection Duration	1.78/1.78	CA
Injection Pressure	2050	bar
Ammonia mass per cycle	270.8	mg
Ammonia Start of Injection	-335	CA ATDC
Ammonia Injection Duration	102	CA
Lambda[1]	1.2	
EGR Rate[2]	0	%

[1]Diesel Definition of EGR

Table 17. Optimized Ammonia RCCI Performance

Parameter	Value	Units
Peak Pressure	194.1	bar
Peak Pressure Angle	15.6	CA
Peak Pressure Rise Rate	5.6	Bar/CA
CA10	3.6	CA
CA50	11.8	CA
CA90	18.3	CA
Burn duration	14.7	CA

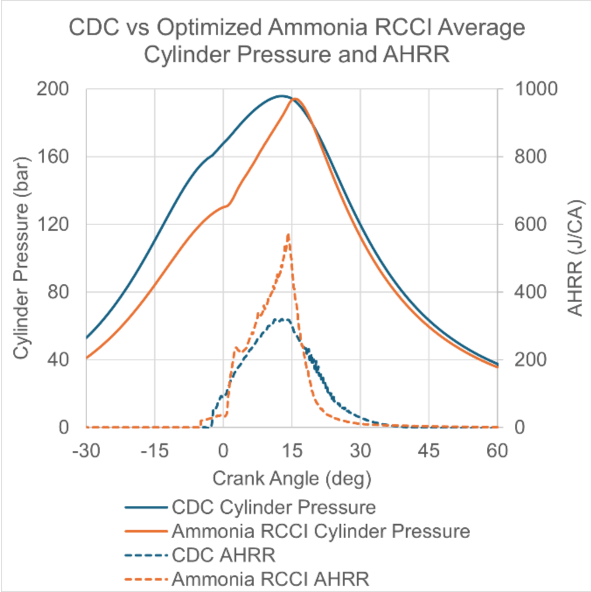

Figure 28. Cylinder pressure comparison of CDC and optimized Ammonia RCCI

5 CONCLUSION

As outlined by Curran et.al [13], a marine engine industry white a paper on the future of ship engines, there is general consensus that both methanol and ammonia, along with traditional LNG are promising fuels for long-haul transportation. In our own on-engine testing and working with partner OEMs on methanol and ammonia dual-fuel engine development, the authors have found common challenges and potentially avoidable pitfalls. This paper and the studies here-in are an attempt to help others benefit from our experience and minimize the efforts required to develop low carbon dual-fuel engines.

Through CFD analysis of the base diesel engine it has been demonstrated that without modification of the combustion strategy both ammonia and methanol perform poorly as a secondary fuel but with proper injection and alterations to the combustion strategy they have the potential to match and exceed the baseline diesel configurations performance, as shown in Table 18. From an engine combustion only point of view, these strategies could result in a reduction of engine-out carbon emissions of 90% while maintaining the engine's geometry and allowing for full diesel backup if required. It should be noted that RCCI requires Active Combustion Control (ACC) using combustion feedback and cycle by cycle diesel SOI control.

Table 18. Compare optimized dual-fuel to diesel baseline

Fuel	Indicated Efficiency (%)	CA50 (deg)	Burn Duration (deg)	Total Heat Release (Joules)
Diesel	45.1	13.0	22.1	5435
Diesel-Ammonia	46.0	11.8	14.7	5478
Diesel-Methanol	46.9	12.4	11.8	5286

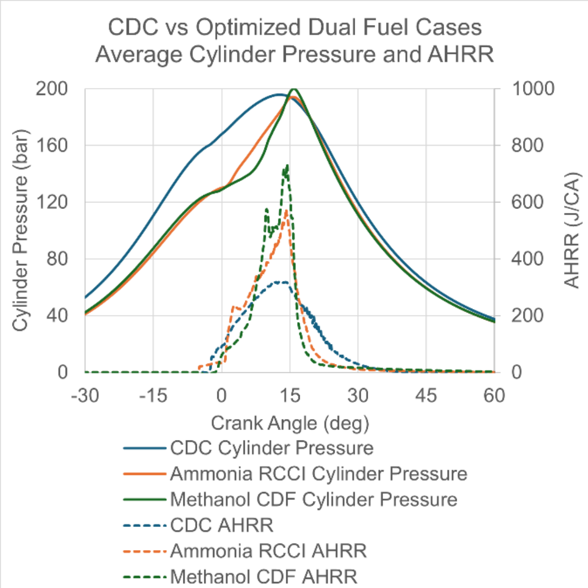

Figure 29. Comparison of optimized dual-fuel pressure traces to base CDC case

Ammonia-Diesel. Woodward tested diesel dual-fuel RCCI on our MTU-4000 engine for both natural gas [5] and for ammonia [4]. The CFD results shown here line up with our experimental experience, especially the need to run richer and use higher back-pressure to increase the residual gases and the charge temperature upon compression.

Methanol-Diesel. It is shown that the methanol injection strategy has a large effect on engine performance. Without leveraging the evaporative cooling of methanol, engine modifications would be needed to lower the compression ratio. A DI injection strategy is strongly preferred due to fewer injection window limitations and increased potential to extract energy from the charge rather than from the engine surfaces. The ideal PFI case requires targeting the back of the intake valve causing the energy required to evaporate the fuel being pulled from the intake runner and intake valve. Extracting the energy for vaporization from the charge also removes the need for an energy source to "pre-vaporize" the methanol to limit wall film accumulation affecting transient performance and engine life due to the solvent/corrosive nature of methanol.

In application, it is known that for many large engines a DI strategy is not feasible and the assumed fuel pressures used in the above paper are not possible due to pump limitations. For these cases where lower fuel pressures and a PFI injection strategy are needed, studious mitigation for methanol wall wetting is required. This can be achieved through detailed spray analysis and injector customization, as detailed above, to minimize distance between injection point and intake valve, optimizing the injection window to the engine's valve profiles and adjusting engine parameters, such as compression ratio, to compensate for diminished evaporative cooling.

For both cases the simple models, while a useful tool for directional improvement, underpredicted the reactivity of the charge in the optimized configurations. This can be attributed to the non-homogenous fuel distribution, trapped hot residuals and radicals from previous cycles.

Future Plans. These concepts will be tested at the Woodward Technology Center on the engine geometry described above.

6 DEFINITIONS, ACRONYMS, ABBREVIATIONS

AFR – Air Fuel Ratio

CA – Crank Angle

BD – Burn Duration

ATDC – After Top Dead Center

BTDC – Before Top Dead Center

CDC – Conventional Diesel Combustion

CDF – Conventional Dual-fuel

CFD – Computation Fluid Dynamics

COV – Coefficient of Variation

RCCI – Reactivity Controlled Compression Ignition

EGR – Exhaust Gas Recirculation

IVC – Intake Valve Close

IVO – Intake Valve Open

EVC – Exhaust Valve Close

EVO – Exhaust Valve Open

SOI – Start of Injection

EOI – End of Injection

dSOI – Diesel Start of Injection

dEOI – Diesel End of Injection

TDC – Top Dead Center

BDC – Bottom Dead Center

7 ACKNOWLEDGEMENTS

Thank you to John Deere for supplying the base model, extensive engine information and test engine! Thank you to John Karspeck for all his

work setting up, maintaining and improving the hardware these simulations were run on.

8 REFERENCES AND BIBLIOGRAPHY

[1] Niki, Y., Nitta, Y, Sekiguchi, H. and Hirata, K. "Emission and Combustion Characteristics of Diesel Engine Fumigated With Ammonia." *ASME 2018 ICE Fall Technical Conference*. San Diego, California, USA. Volume 1: Large Bore Engines; Fuels; Advanced Combustion.

[2] Liu S., Sun T., Zhou L., Jia M., Zhao W. and Wei H. 2023. A new skeletal kinetic model for methanol/ n-heptane dual-fuels under engine-like conditions, *Energy*, Volume 263, Part 2.

[3] Xu L., Chang Y., Treacy M., Zhou Y., Jia M. and Bai X. 2023. A skeletal chemical kinetic mechanism for ammonia/n-heptane combustion, *Fuel*, Volume 331, Part 2.

[4] Chiera, D., Wood, J., Jones, A., Polley, N., Buehner, M. and Hampson, G.J. 2022. Method to Reach High Substitution of an Ammonia Fueled Engine Using Dual-fuel RCCI and Active Combustion Control, *ASME Fall Internal Combustion Engine Conference*, ASME, Indianapolis, Indiana, USA, ICEF2022-88759

[5] Chiera, D., Wood, J., Polley, N., Buehner, M. and Hampson, G.J. 2021. Active Combustion Controlled Diesel/Natural Gas in RCCI mode to Reduce Methane Emissions in Lean Burn Engines, *18th Symposium, Sustainable Mobility, Transport and Power Generation*, Institute of Internal Combustion Engines and Thermodynamics, Graz University of Technology, Graz, Austria.

[6] Chiera, D., Wood, J., Polley, N., Buehner, M. and Hampson, G.J. 2021. Strategies to Reduce Methane Slip in Natural Gas Diesel Dual-fuel Marine and Power Generation Engines, *Internal Combustion Engine Fall Conference*

[7] Nordin, N. 1998. *Numerical Simulations of Non-Steady Spray Combustion Using a Detailed Chemistry Approach Thesis for the degree of Licentiate of Engineering, Dept. of Thermo and Fluid Dynamics*, Chalmers University of Technology, Goteborg, Sweden

[8] Stagni, A., Cavallotti, C., Arunthanayothin, S., Song, Y., Herbinet, O., Battin-Leclerc, F. and Faravelli, T. 2020. An experimental, theoretical and kinetic-modeling study of the gas-phase oxidation of ammonia. *Reaction Chemistry & Engineering*, 5, 696-711.

[9] Siong Chai, W., Bao, Y., Jin, P., Tang, G. and Zhou, L. 2021. A review on ammonia, ammonia-hydrogen and ammonia-methane fuels, *Renewable and Sustainable Energy Reviews*, Volume 147

[10] Yousefi, A., Guo, H., Dev, S., Lafrance, S. and Liko, B. 2022. A study on split diesel injection on thermal efficiency and emissions of an ammonia/diesel dual-fuel engine. *Fuel,* Volume 316

[11] Dodge L, and Naegeli D. 1994. *Injector Spray Characterization of Methanol in Reciprocating Engines*, Southwest Research Institute, San Antonio, USA

[12] Willmann, M., Wood, J., Barow, E., Berger, I. 2023. PtX fuels for combustion engines: flexible injection concepts for all applications, 30th *CIMAC World Congress,* Busan, South Korea

[13] Curran S, Onorati A, Payri R, Hampson G.J., et al. 2024. The future of ship engines: Renewable fuels and enabling technologies for decarbonization. *International Journal of Engine Research*, 25(1), 85-110.